THE ASTROPHYSICAL JOURNAL, 456:451–465, 1996 January 10

SOFT X-RAY OBSERVATIONS OF A COMPLETE SAMPLE OF X-RAY–SELECTED BL LACERTAE OBJECTS

ERIC S. PERLMAN,[1] JOHN T. STOCKE, AND Q. DANIEL WANG[2]
Center for Astrophysics and Space Astronomy, Campus Box 389, University of Colorado, Boulder, CO 80309

AND

SIMON L. MORRIS
Dominion Astrophysical Observatory, Herzberg Institute for Astrophysics, 5071 W. Saanich Road, Victoria, BC, Canada V8X 4M6

Received 1994 September 29; accepted 1995 July 21

ABSTRACT

We present the results of *ROSAT* PSPC observations of the X-ray selected BL Lacertae objects (XBLs) in the complete *Einstein* Extended Medium Sensitivity Survey (EMMS) sample. None of the objects is resolved in their respective PSPC images, but all are easily detected. All BL Lac objects in this sample are well-fitted by single power laws. Their X-ray spectra exhibit a variety of spectral slopes, with best-fit energy power-law spectral indices between $\alpha = 0.5$–2.3. The PSPC spectra of this sample are slightly steeper than those typical of flat ratio-spectrum quasars. Because almost all of the individual PSPC spectral indices are equal to or slightly steeper than the overall optical to X-ray spectral indices for these same objects, we infer that BL Lac soft X-ray continua are dominated by steep-spectrum synchrotron radiation from a broad X-ray jet, rather than flat-spectrum inverse Compton radiation linked to the narrower radio/millimeter jet.

The softness of the X-ray spectra of these XBLs revives the possibility proposed by Guilbert, Fabian, & McCray (1983) that BL Lac objects are lineless because the circumnuclear gas cannot be heated sufficiently to permit two stable gas phases, the cooler of which would comprise the broad emission-line clouds. Because unified schemes predict that hard self-Compton radiation is beamed only into a small solid angle in BL Lac objects, the steep-spectrum synchrotron tail controls the temperature of the circumnuclear gas at $r \leq 10^{18}$ cm and prevents broad-line cloud formation.

We use these new *ROSAT* data to recalculate the X-ray luminosity function and cosmological evolution of the complete EMSS sample by determining accurate K-corrections for the sample and estimating the effects of variability and the possibility of incompleteness in the sample. Our analysis confirms that XBLs are evolving "negatively," opposite in sense to quasars, with $\langle V_e/V_a \rangle = 0.331 \pm 0.060$. The statistically significant difference between the $\langle V_e/V_a \rangle$ values for X-ray and radio-selected BL Lac objects remains a difficulty for models which unify these two types of objects. We have identified one addition to the sample, so that the sample now has 23 objects. We find no evidence for a substantial number of unidentified low-luminosity BL Lac objects hidden in our sample, as had been suggested by Browne & Marcha (1993) although a few such objects may be present.

Subject headings: BL Lacertae objects: general — galaxies: evolution — galaxies: luminosity function — X-rays: galaxies

1. INTRODUCTION

BL Lac objects are characterized by "featureless" spectra which are dominated by an overall parabolic (in νF_ν) continuum through several decades in frequency (Giommi, Ansari, & Micol 1995; Antonucci 1993 and sources therein). They are copious emitters in the X-ray, with observed X-ray luminosities $\log L_x = 44$–46 (ergs s^{-1}; Morris et al. 1991, hereafter M91; Schwartz & Ku 1983; here and elsewhere in this paper we present luminosities as integrated over 4π steradians). The overall spectral shapes of BL Lac objects are unique, occupying a distinct area in a radio/optical/X-ray color-color diagram. This provides an efficient method of finding these enigmatic objects (Stocke et al. 1989; Schachter et al. 1993; Perlman et al. 1995).

BL Lacertae objects share a number of properties which directly indicate that their unique properties are a result of seeing a relativistically beamed jet very close to the line of sight. For example, many are superluminal sources (see Vermeulen & Cohen 1994 for a comprehensive list of superluminal objects); further, the γ-ray emissions found in nine BL Lac objects by EGRET require $\Gamma \gtrsim 5$ in order to avoid the quenching of γ-ray emission through pair production (Mattox et al. 1993). In addition, BL Lacs are highly polarized, and many have wildly varying position angles of polarization, suggesting that we are looking nearly directly along the axis of a wiggling or precessing relativistic jet (Blandford & Konigl 1979). Hypotheses which invoke relativistic beaming to explain BL Lac properties are often called "unified schemes." Under unified schemes a parent population, i.e., objects which, if beamed, would produced BL Lacs, is needed; most often Fanaroff-Riley type 1 (F-R 1; Fanaroff & Riley 1974) radio sources are invoked (Padovani & Urry 1990, 1991) and are consistent with most current data.

The observed space density of X-ray selected BL Lacertae

[1] Currently USRA Visiting Scientist, Goddard Space Flight Center, Code 668, Greenbelt, MD 20771; e-mail: perlman@rosserv.gsfc.nasa.gov.
[2] Currently Department of Physics and Astronomy, Northwestern University, 2145 N. Sheridan Road, Evanston, IL 60208-3112.

objects (XBLs)[3] is $\gtrsim 10$ times greater than that of radio-selected BL Lacs (RBLs) (Wolter et al. 1994; Padovani & Urry 1990). They also possess somewhat larger starlight fractions within their optical spectra (M91) and larger galaxy fractions in their optical images (Wurtz 1994) than do RBLs (Stickel, Fried, & Kühr 1993; Abraham, McHardy, & Crawford 1991). XBLs display less extreme variability and polarization properties than RBLs (Jannuzi, Smith, & Elston 1993, 1994), and many XBLs display preferred position angles of polarization (Jannuzi et al. 1994), which RBLs rarely exhibit. Hypotheses which attempt to unify XBLs and RBLs as a single population must therefore explain these differences.

A detailed discussion of unified scheme models is beyond the scope of this paper; here we briefly review the two leading models unifying XBLs and RBLs. In one (known as the "viewing angle" hypothesis), XBLs are seen farther from the beaming axis than are RBLs (e.g., Browne 1983, 1989; Padovani & Urry 1990, 1991; Urry, Padovani, & Stickel 1991; Ghisellini et al. 1993; Celotti et al. 1993), thus requiring the X-ray emitting material to be less collimated than the radio emission region (Stocke et al. 1989; Padovani & Urry 1990, 1991; Urry et al. 1991; Ghisellini et al. 1993). This hypothesis has the virtue of explaining the observed number counts as a natural consequence of the solid angle through which they are viewed; however, Sambruna (1994) has recently pointed out that it has difficulty explaining some facets of the multiwavelength spectra of XBLs and RBLs.

An alternative model (which we will refer to as the "energy cutoff" model) has been proposed by Giommi & Padovani (1994; also see Padovani & Giommi 1995; Giommi et al. 1995) under which BL Lacs are a single population with a continuum of energy cutoffs. Here XBLs are that minority of BL Lacs with cutoff energies in the UV or X-rays (compared to RBLs, which have cutoffs in the optical or IR), and are intrinsically less powerful in the radio. As a result, the observed number counts (Wolter et al. 1991, 1994) must be explained as a selection effect. This scheme has the virtue that the luminosity function, log N-log S and radio flux distributions of XBLs can be derived from those of RBLs. However, it does not give a physical reason for the differences in overall spectral shapes; nor can it easily explain the preferred position angles of polarization observed for most XBLs (Jannuzi et al. 1994).

Both models agree that the X-ray luminosity function of BL Lac objects is consistent with a beamed population of F-R 1's (Padovani & Urry 1990; M91). An isotropic component of BL Lac X-ray emission cannot be ruled out presently (Madejski & Schwartz 1989), but is likely very weak, as suggested by the recent detection of weak point X-ray sources in F-R 1 radio galaxies by Worrall & Burkinshaw (1994). It is therefore unclear why the XBL population exhibits "negative" evolution (§ 5; Maccacaro et al. 1984; M91; Wolter et al. 1994), with $\langle V/V_{\rm max}\rangle = 0.331 \pm 0.060$, while the RBL population is consistent with either "positive" or no evolution at the 2 σ level with $\langle V/V_{\rm max}\rangle = 0.60 \pm 0.05$ (1 Jy sample; Stickel et al. 1991). The difference between these values remains a problem for unified schemes.

[3] While the terms XBL and RBL historically refer to the discovery method, this leaves several bright BL Lacs as both XBLs and RBLs. Therefore, in this paper, we adopt the definition of Wurtz (1994), based upon the ratio of X-ray to radio flux. The dividing line between XBLs and RBLs is set at $\log f_x/f_r \approx -5.5$, where the X-ray flux (in Jy) is measured at 1 keV, and the radio flux (in Jy) at 5 GHz. A similar formulation has been suggested by Giommi & Padovani (1994).

Previously the X-ray galaxies of BL Lacs were based on *Einstein* IPC or *EXOSAT* CMA data which often did not tightly constrain the spectral index α (where $F \propto E^{-\alpha}$) (Worrall & Wilkes 1990; Barr et al. 1989; Sambruna et al. 1994a, b). Therefore, given the potential importance that X-ray emission could play in constraining physical models for BL Lacs (e.g., Guilbert, Fabian, & McCray 1983; hereafter GFM83), we observed the complete EMSS sample of XBLs (as defined in M91) with the *ROSAT* PSPC, obtaining both images and low-resolution spectroscopy. A companion study will examine the X-ray spectra for a complete sample of RBLs from the 1 Jy sample (Sambruna 1994; Urry et al. 1996). We also use these data to determine the effect of the K-correction on the luminosity function and $\langle V/V_{\rm max}\rangle$ value for XBLs. Despite the fairly steep spectra, the K-corrections are small (see § 5) due to the modest redshifts of the objects in the EMSS XBL sample.

Our data confirm that X-ray selected BL Lacs are undergoing "negative" evolution, and further, establish that their soft X-ray spectra are mostly steep, with a wide spread in power-law spectral indices, $0.5 \lesssim \alpha \lesssim 2.3$. The median value is $\alpha = 1.32$. Earlier work assumed $\alpha = 1$ for this sample, based on a maximum likelihood analysis of the *Einstein* IPC spectral indices for a sample of BL Lacs (Worrall & Wilkes 1990).

Recent work (Sambruna 1994; Urry et al. 1996) shows that the PSPC X-ray spectra of RBLs are similarly steep. Thus any XBL/RBL differences must occur at higher energies than the PSPC was sensitive to. Particularly relevant in this respect are the results of Ciliegi, Bassani, & Caroli (1995), who note that the canonical X-ray spectrum for XBLs tends to steepen slightly at 2–10 keV, while the canonical RBL spectrum tends to flatten significantly over the same energy range (in line with predictions we make in § 4). We will attempt to construct a consistent picture for the X-ray spectra of BL Lacs out of these past results and the current data.

All work in this paper assumes $H_0 = 50$ km s^{-1} Mpc^{-1} and $q_0 = 0$. Except where noted, all error bars quoted are 90% confidence.

In § 2, we describe the observations and data reduction process, including the fitting of single power-law plus absorption models to the PSPC spectra. In § 3, we compare these results with X-ray spectra for various classes of active galactic nuclei (AGNs), including RBLs, F-R 1 radio galaxies, and quasars. In § 4, we discuss the steepness of BL Lac X-ray spectra, including both the implications of this result for the suppression of a broad-line region in BL Lacs, and its implications for unified schemes. In § 5, we use the new spectral indices to reexamine the X-ray luminosity function and cosmological evolution for the EMSS XBL sample, and we consider the implications of X-ray variability. We also evaluate the possible incompleteness of the sample. Finally, in § 6, we summarize our findings.

2. OBSERVATIONS AND DATA REDUCTION

ROSAT PSPC data were obtained for all 22 objects in the complete EMSS sample of XBLs as defined in M91 (finding charts for the EMSS BL Lacs can be found in Maccacaro et al. 1994). A log of the observations and basic data extracted from the PSPC observations are presented in Table 1. Given that the errors in most of the listed spectral indices are quite modest, the spread in spectral slopes is real. For 16 of the objects, we were able to carry out pointed observations. In the case of another three (indicated by O in Table 1), we obtained

TABLE 1

LOG OF OBSERVATIONS AND BASIC DATA

Object (1)	Exposure (s) (2)	Counts (3)	α (90% conf. errors) (4)	N(H) (cm^{-2}) (5)	Galactic N_H[a] (cm^{-2}) (6)	F(0.1–2.4 keV) (10^{-13} ergs cm^{-2} s^{-1}) (7)	χ_ν(DOF)[b] (8)	P_F (9)	Notes (10)
MS 0122.1+0903.....	11173	181	$0.62^{+0.44}_{-0.55}$	4.90	4.90	1.93	0.764 (26)		
MS 0158.5+0019.....	1646	1107	$1.46^{+0.23}_{-0.31}$	$2.88^{+0.65}_{-0.59}$	2.00	61.45	2.135 (27)	>95%	
MS 0205.7+3509.....	13964	2604	$1.71^{+0.23}_{-0.21}$	$26.40^{+4.3}_{-3.2}$	6.10	23.67	1.073 (27)	>99.9%	1
MS 0257.9+3429.....	7434	230	$1.67^{+0.30}_{-0.33}$	9.90	9.90	3.54	1.196 (28)		
MS 0317.0+1834.....	2917	409	$1.32^{+0.23}_{-0.25}$	10.00	10.00	17.20	1.252 (28)		
MS 0419.3+1943.....	4704	683	$0.72^{+0.26}_{-0.27}$	19.00	19.00	19.78	0.850 (28)		2
MS 0607.9+7108.....	14086	249	$1.21^{+0.30}_{-0.34}$	8.10	8.10	2.37	0.954 (28)		3
MS 0737.9+7441.....	455.7	223	0.91	3.20	3.20	48.94			4
MS 0922.9+7459.....	4137	399	$0.78^{+0.13}_{-0.14}$	2.10	2.10	10.01	0.791 (28)		
MS 0950.9+4929.....	3669	1136	$1.76^{+0.26}_{-0.24}$	$1.58^{+0.55}_{-0.45}$	0.92	18.34	1.342 (28)	>90%	
MS 1019.0+5139.....	564.8	265	0.52	0.95	0.95	47.19			4
MS 1207.9+3945.....	38127	8166	$1.13^{+0.10}_{-0.09}$	$3.54^{+0.32}_{-0.35}$	2.10	23.51	1.429 (27)	>99.9%	3
MS 1221.8+2452.....	5642	833	$1.47^{+0.29}_{-0.26}$	$1.76^{+0.71}_{-0.58}$	1.60	11.13	0758 (27)		2
MS 1229.2+6430.....	3034	2483	0.99 ± 0.15	$2.97^{+0.48}_{-0.45}$	2.00	92.40	0.722 (27)	>99.9%	
MS 1235.4+6315.....	3204	596	1.91 ± 0.08	$2.29^{+1.09}_{-0.91}$	1.70	12.75			5
MS 1402.3+0416.....	4763	2870	1.85 ± 0.17	$2.30^{+0.40}_{-0.37}$	2.20	44.46	1.232 (27)		2
MS 1407.9+5954.....	4120	432	1.74 ± 0.14	1.60	1.60	6.71	1.257 (28)		3
MS 1443.5+6348.....	4208	663	$1.10^{+0.30}_{-0.28}$	$2.88^{+0.94}_{-0.85}$	1.70	16.10	1.288 (27)	>90%	
MS 1458.8+2249.....	4557	1686	$2.31^{+0.22}_{-0.19}$	$5.83^{+0.68}_{-0.67}$	3.40	40.39	1.464 (27)	>99.9%	
MS 1534.2+0148.....	2380	583	$0.89^{+0.17}_{-0.18}$	4.60	4.60	29.96	0.788 (28)		
MS 1552.1+2020.....	3652	2919	0.79 ± 0.14	$4.23^{+0.56}_{-0.55}$	3.90	105.59	1.484 (25)		2
MS 1757.7+7034.....	5169	1801	1.12 ± 0.13	3.65 ± 0.43	4.60	39.50			4[b]
MS 2143.4+0704.....	3526	741	$1.91^{+0.34}_{-0.31}$	$10.76^{+3.49}_{-2.02}$	4.80	25.13	1.605 (27)	>99.9%	

[a] Galactic N_H data from Gioia et al. 1990.

[b] 1 σ errors only were provided by Fleming (private communication).

NOTES.—(1) Fit assumes absorption at $z = 0.318$ (see text). (2) χ^2 statistic from both fitting procedures were comparable. (3) Off-axis observation. (4) Data from *ROSAT* All-Sky Survey. (5) Data provided by H.-C. Thomas, private communication.

PSPC data from observations pointed at nearby targets within the PSPC field of view. One EMSS XBL (MS 1235.4+6315) was the target of a PSPC observation made by H.-C. Thomas, who kindly forwarded his results to us so that they could be included here (indicated by T in Table 1). For two BL Lacs (MS 1757.7+7034 and MS 0737.9+7441), spectra were extracted from the *ROSAT* all-sky survey images (indicated by R in Table 1) by S. Molendi et al. (in preparation) and kindly communicated to us prior to publication. Finally, we have added one probable XBL to the sample (MS 1019.0+5139; see § 5.2 for details), for which RASS data (Molendi et al., in preparation) were used.

2.1. *Extraction and Spectral Fitting*

For the pointed observations, soft X-ray spectra were produced by using a 2′ extraction radius for source photons, and a 2′.5–5′ annulus for the background photons. In two cases, where other sources were found inside the background extraction annulus, the confusing sources were excluded by changing the dimensions of the annulus, rather than via a source mask. The standard IRAF binning procedure was used, and spectra were fitted to channels 3–32, except in the case of MS 0122.1+0903 and MS 1552.1+2020, where only channels 3–30 were fitted. The spectra were fitted with single power-law models plus a Morrison-McCammon absorption model. For all data in which the BL Lac object was the target of the observation, extractions were performed in the IRAF X-ray/PROS package and all fits were performed in XSPEC version 8.5. The data for these objects was reextracted and refitted following the discovery of error-handling problems in PROS. For pointed data taken in "high-gain" mode (before 1991 October 14), the 1992 March 11, matrix was used, while for data taken after 1991 October 14 (e.g., in "low-gain" mode), the 1993 January 12, response matrix was used. For MS 0737.9+7441 and MS 1019.0+5139, spectra were derived from the hardness ratio analysis (S. Molendi, private communication), while for MS 1757.7+7034 a fit in XSPEC was performed.

In general, we employed two fitting procedures: first, we allowed both the spectral index α and the absorbing column N_H to vary freely; in the second, we fixed the absorbing column at Galactic values (Gioia et al. 1990b; Stark et al. 1992), allowing only the spectral index to vary. This allowed us not only to gauge which fitting procedure produced the best fit, but also to check whether in any case there was convincing evidence for excess absorption above Galactic values (§ 2.2). To compare the fits yielded by these two procedures, the F-test was used (e.g., Bevington & Robinson 1992). Also, we visually inspected the data and errors thus produced to judge whether the fits produced adequately constrained the parameters, even if the F-test produced a result verifying that the extra parameter was justified. In Table 1, columns (7) and (8) list statistics used to judge the goodness of fit. Column (7) contains the reduced χ^2 values, and in parentheses the degrees of freedom. Column (8) lists the F-test probability that the fitting procedure which best describes the PSPC data is the one where N_H is not fixed at the Stark et al. (1992) value but rather is allowed to vary.

After comparing the fits yielded by the two procedures above, we determined that models for these spectra sufficiently constrained both α and N_H only if $\gtrsim$600 counts were present. We considered a fit adequately constrained by the data if the error bars on α were $\lesssim$0.4 and the error bars on N_H were

$\lesssim$40%. For a typical spectrum with $\sim$400 counts, models with both α and N_H free produced error bars on $\alpha \sim 1$, and similarly poorly constrained fits for N_H. Thus, for objects with less than 600 counts (Table 1), we quote the results of the fitting procedure where both α and N_H were allowed to vary. For all objects, we present (for comparison) the Galactic value of N_H as given in Gioia et al. (1990b).

The exceptions to this rule are MS 0419.3+1943 and MS 1534.2+0148. For MS 0419.3+1943 (683 counts), the fitting procedure which allowed both α and N_H to vary did not adequately constrain the data (achieving $\alpha = 0.27^{+1.07}_{-0.43}$ and $N_H = 10.29^{+19.58}_{-4.51} \times 10^{20}$ cm^{-2}). For MS 1534.2+0148 (583 counts), the two fitting procedures produced comparable values of χ^2. However, when both α and N_H were left as free parameters, they were not well constrained by the data ($\alpha = 0.96^{+0.44}_{-0.45}$ and $N_H = 4.91^{+1.79}_{-1.47} \times 10^{20}$ cm^{-2}). For both objects we quote in Table 1 the best-fit spectral index achieved using the fixed-N_H procedure.

For four objects we were unable to directly compare the fits produced by these two procedures. The objects are MS 0737.9+7441, MS 1019.0+5139, MS 1235.4+6315, and MS 1757.7+7034. For MS 1235.4+6315, H.-C. Thomas has allowed us the use of his results prior to publication. These results were achieved by allowing both α and N_H to vary and are quoted in Table 1; however, we have no other particulars (including χ^2 values). For the remaining three sources, only RASS data exist. For MS 0737.9+7441 and MS 1019.0+5139, S. Molendi et al. (in preparation) calculated a spectral index fit to the observed hardness ratio assuming Galactic N_H. For MS 1757.7+7034, which has greater than 1700 counts in the RASS data, T. Fleming (private communication) performed a fit in XSPEC allowing both α and N_H to vary; those results are quoted in Table 1.

We present in Figure 1 four representative extracted spectra, along with fitted models for the α and N_H values listed in Table 1. In Figure 2, we present χ^2 grids in the (α, N_H) plane for two objects. Plots of the extracted spectra, fits, and χ^2 grids for the entire sample may be found in Perlman (1994). The fitted spectral indices fall in the range $0.5 \lesssim \alpha \lesssim 2.3$, with a median of $\alpha = 1.32$. The mean spectral index is $\alpha = 1.30 \pm 0.48$ (68% confidence). One object has $\alpha > 2$ (MS 1458.8+2249). In 22 of 23 cases, the value of $Q(\chi^2 \mid \nu)$, the probability of exceeding the listed value of χ^2 by chance is less than 95% (values of $Q(\chi^2 \mid \nu)$ are tabulated by, for example, Abramowitz & Stegun 1964, pp. 975–985). For these objects, a power law plus the quoted value of N_H (Table 1) is an adequate fit to the data. The best-fit values are listed in Table 1.

For one object, MS 0158.5+0019, the fitting procedures did not converge adequately; neither did alternate models, such as thermal bremsstrahlung or broken power laws, produce adequate fits. As listed in Table 1, the best fit $\chi^2 = 2.135$, e.g., $Q(\chi^2 \mid \nu) = 0.9995$, for the power-law model shown. The

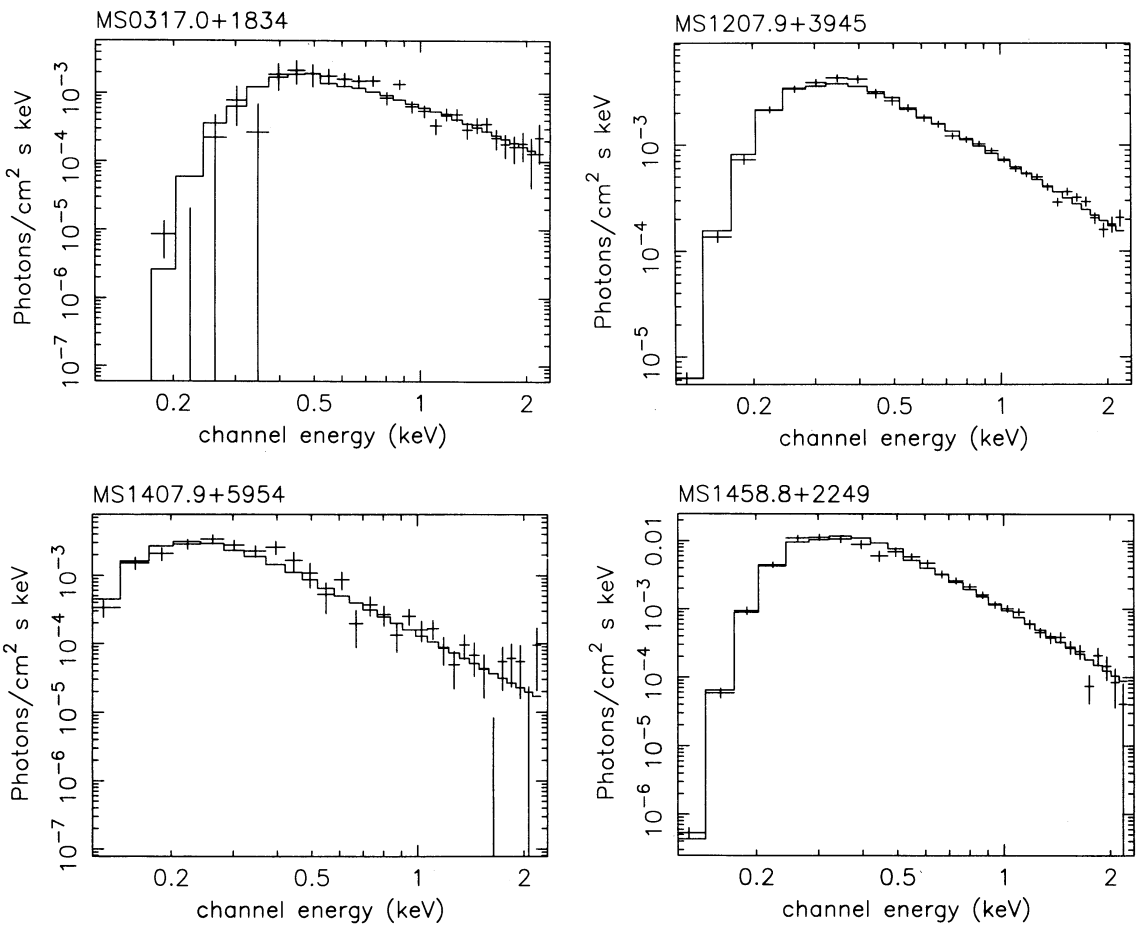

FIG. 1.—*ROSAT* PSPC spectra and fits for four representative EMSS XBLs. In each spectrum, we show (1) the received spectrum (*pluses*), and (2) the model predictions (*histogram*). See § 2 and Table 1 for details.

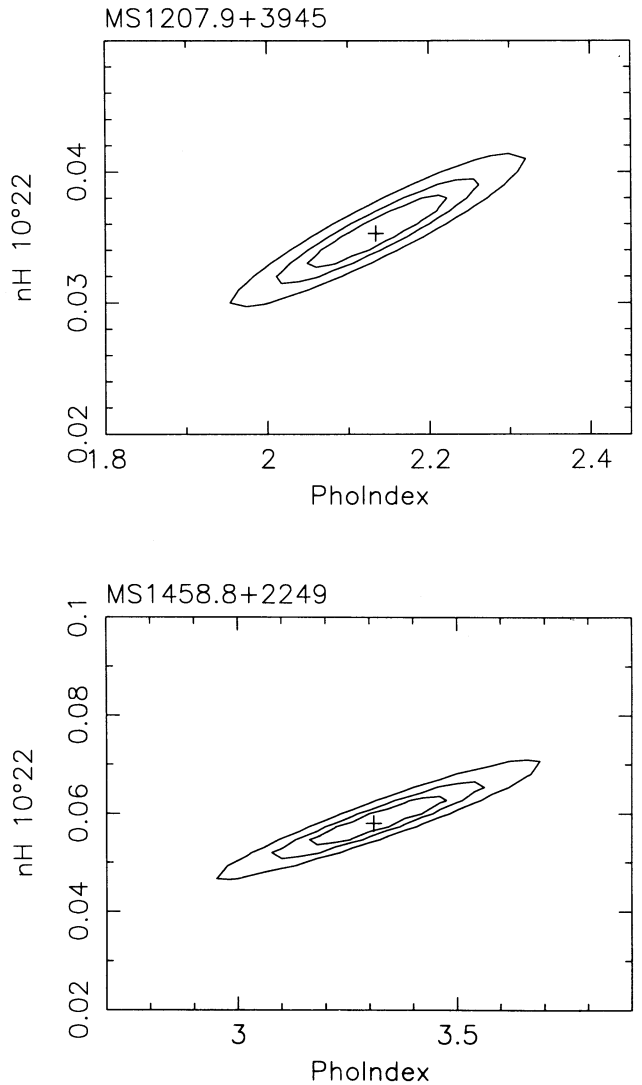

FIG. 2.—χ^2 contour plots for two representative EMSS XBLs. The χ^2 confidence contours of the fit are at the 68%, 90%, and 99% confidence levels. See § 2 and Table 1 for details.

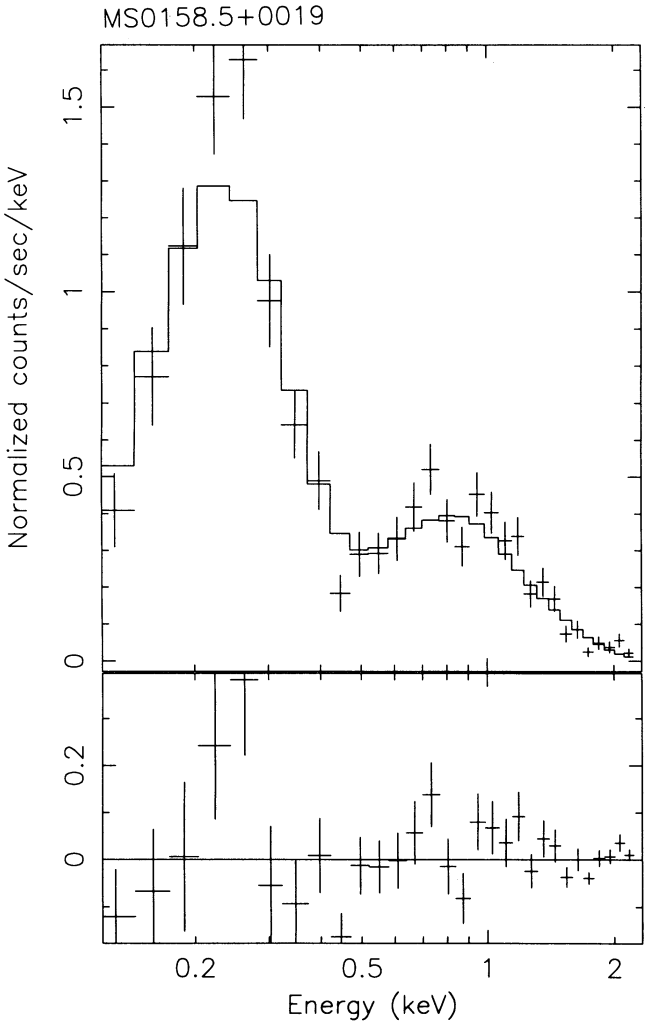

FIG. 3.—Spectrum and residuals from the fits for MS 0158.5+0019. Notice that the departures which cause the large χ^2 are seen in only a few nonadjacent channels, suggesting poor background subtraction.

residuals for this object are shown in Figure 3. As can be seen, the departures are concentrated in a few nonadjacent channels, possibly suggesting poor background subtraction. This hypothesis is supported by the presence of a confusing X-ray source $\approx 2'.5$ away from the BL Lac which was difficult to exclude from both the source extraction and background extraction regions. A number of extraction procedures were tried; none completely eliminated this effect. We therefore believe that the data for MS 0158.5+0019 could not be fitted adequately as a result of confusing photons from a nearby X-ray source which was poorly subtracted from the background.

The PSPC spectral indices and N_H values derived in this paper have been used to rederive EMSS IPC fluxes for these sources. Because Gioia et al. (1990b) assumed $\alpha = 1$ to compute the flux of these sources, we have derived new discovery fluxes and 1 σ Poissonian errors (listed in Table 2) based upon their actual soft X-ray spectral indices. For this calculation, we used PIMMS to recalculate the fluxes based on those spectral indices and Galactic N_H values, combined with IPC count rates and errors from Gioia et al. (1990b). The assumption of Galactic absorption causes errors $\lesssim 20\%$ for a few sources, where the F-test indicates that fits with N_H fixed at Galactic (Stark et al. 1992) levels were inadequate. However, sky coverages for the EMSS have been calculated assuming Galactic N_H (Gioia et al. 1990b). The most exact treatment would calculate the sky coverage of the EMSS in source counts rather than flux given the possibility of extra intrinsic absorption in any given source. Because only two sources exhibit excess absorption above Galactic values (§ 2.2), this effect is quite minor (see also Maccacaro et al. 1984).

We caution that our recalculation of IPC discovery fluxes for the EMSS sample of XBLs does not account for the effects of variability on the X-ray spectrum. BL Lac spectra have been observed to harden when in a high state (Giommi et al. 1991). Indeed, there is evidence from *EXOSAT* observations (Sambruna et al. 1994a) that two objects in this sample follow this trend (MS 0317.0+1834 and MS 1402.3+0416; see § 3). The effect of variability upon the X-ray luminosity function is covered in § 5.1.

We also fitted Gaussian image profiles to each BL Lac image, in order to determine if the object was resolved. All

TABLE 2

RECALCULATED IPC FLUXES

Object	IPC Flux[a]
MS 0122.1+0903.....	8.23 ± 0.95
MS 0158.5+0019.....	80.68 ± 5.72
MS 0205.7+3509.....	6.48 ± 1.40
MS 0257.9+3429.....	16.47 ± 3.92
MS 0317.0+1834.....	148.74 ± 8.49
MS 0419.3+1943.....	26.94 ± 17.22
MS 0607.9+7108.....	15.13 ± 2.40
MS 0737.9+7441.....	108.18 ± 6.11
MS 0922.9+7459.....	12.34 ± 1.43
MS 0950.9+4929.....	24.14 ± 3.06
MS 1019.0+5139.....	16.99 ± 2.13
MS 1207.9+3945.....	15.45 ± 0.54
MS 1221.8+2452.....	10.46 ± 1.34
MS 1229.2+6430.....	36.61 ± 2.91
MS 1235.4+6315.....	13.62 ± 1.05
MS 1402.3+0416.....	9.35 ± 0.59
MS 1407.9+5954.....	15.26 ± 1.15
MS 1443.5+6348.....	16.49 ± 1.45
MS 1458.8+2249.....	9.57 ± 0.88
MS 1534.2+0148.....	23.03 ± 2.20
MS 1552.1+2020.....	48.73 ± 2.82
MS 1757.7+7034.....	26.35 ± 3.18
MS 2143.4+0704.....	25.83 ± 5.38

[a] In units, $\times 10^{-13}$ ergs cm^{-2} s^{-1}

sources were found to be adequately represented by Gaussians of FWHM $\leq 15''$ size (consistent with the typical size for the PSPC point-response function; Hasinger et al. 1992) at the position of the radio and optical source to within the expected errors on the X-ray position ($\sim \pm 10''$, Hasinger et al. 1992). Even for the two EMSS XBLs known to be in rich clusters of galaxies (MS 1207.9+3945, MS 1407.9+5954; see Wurtz et al. 1993b), and another known to have a foreground cluster in the field (MS 0922.9+7459 has Abell 786 in the field), we did not find evidence for any extended X-ray emission. Gioia et al. (1990b) previously reported that three EMSS BL Lacs had possibly extended emission on the IPC (MS 0257.9+3429, MS 1229.2+6430, and MS 2143.4+0704). However, these objects were at the edge of the IPC field of view; and our data do not show any extended emission in these objects.

2.2. *Comparison of Fitted Hydrogen Columns to Galactic Values*

For all but one source with greater than 600 counts (Table 1), we were able to test whether there is any evidence for excess absorption above Galactic values by the dual-fit procedure described above. In three objects (MS 1207.9+3945, MS 1229.2+6430, and MS 1458.8+2249), the addition of an extra parameter caused by allowing N_H produced a better fit to the data which was significant at the greater than 99.9% level according to the F-test. In two of these cases (MS 1207.9+3945 and MS 1458.8+2249), the fixed N_H fitting procedure did not yield acceptable fits (reduced χ^2 values of 2.86 and 3.61, respectively). For MS 1229.2+6430, the fixed N_H procedure did produce an adequate model ($\chi^2 = 1.15$). But in all three cases, the difference between the best-fit value of N_H and the Galactic (Gioia et al. 1990b; Stark et al. 1992) value was $\lesssim 0.2$ in the log. For these three sources, we find no evidence of excess absorption above Galactic levels.

In only two cases is there convincing evidence for an excess absorbing column (MS 0205.7+3509 and MS 2143.4+0704). The fixed N_H fitting procedure yielded a reduced $\chi^2 = 5.07$ for MS 0205.7+3509, which is clearly unacceptable. By comparison, letting both α and N_H vary we achieved a far more well-constrained fit with a reduced $\chi^2 = 1.07$. The results of the F-test (Table 1) clearly indicate that the extra parameter produced by letting N_H vary is well justified. The Galactic absorbing column listed in Table 1 is well outside the 99% confidence contours in (N_H, α). Given the very large number of counts received for this object (2584), we conclude that this object requires a much higher column density than that quoted by Gioia et al. (1990b).

It is probable that this excess absorbing material is resident in the host galaxy of this object, and not within our Galaxy, as *IRAS* measurements at 100 μm show only small local enhancement ($\delta N_H \approx 1$–2×10^{20} cm^{-2}), not nearly enough to account for the excess soft X-ray absorption we find. MS 0205.7+3509 has a point source which is decentered relative to its "host" galaxy (Wurtz et al. 1993a), making it a prime candidate for a gravitationally lensed system. If the excess absorbing gas is within the visible "host," it is possible that this is an example of a "dusty" gravitational lens, as mentioned by Perlman et al. (1994). See Stocke, Wurtz, & Perlman (1995) for further details. We have therefore assumed that the absorbing gas is at $z = 0.318$, the redshift of the "host" galaxy, for the model shown in Table 1.

Similarly, the fixed-N_H fitting procedure yielded a unacceptable reduced $\chi^2 = 2.73$ for MS 2143.4+0704. Allowing both α and N_H to vary produced a reasonable fit to the data, with $\chi^2 = 1.61$. According to the results of the F-test (Table 1), there is a greater than 99.9% probability that adding the extra parameter to the fit has produced a better model of the data. While this seems to indicate a significantly higher value of N_H than Galactic for MS 2143.4+0704 (by a factor ~ 2), this result is not as clear cut as for MS 0205.7+3509 because the X-ray data do not constrain the fit value of N_H as tightly. Further, MS 2143.4+0704 is at a lower Galactic latitude, where larger small-scale fluctuations in N_H are possible. Therefore, MS 2143.4+0704 possesses possible excess absorption.

Because the Stark et al. (1992) results were achieved with a 1° beam, the exact Galactic column toward these sources is not well known. For example, Elvis, Lockman, & Fassnacht (1989) and Elvis, Wilkes, & Lockman (1994) found many small scale ($\sim$10%–15% at 90% confidence) deviations from the Stark et al. results at high Galactic latitudes. While the best-fit N_H values for these two sources deviate from the Galactic value quoted in Gioia et al. (1990b) by amounts which are much larger than the fluctuations found by Elvis et al. (1989, 1994), we cannot completely discount that the X-ray absorption is Galactic, particularly in the case of MS 2143.4+0704. For the objects for which we give fits with N_H fixed at the Galactic value, we have performed tests in XSPEC to simulate the changes in α and F(0.1–2.4 keV) that such N_H fluctuations would produce. In all cases, any such changes are well within the 90% confidence error bars in α and produced very small differences in the quoted fluxes.

3. COMPARISONS OF OUR DATA WITH EARLIER OBSERVATIONS AND OTHER CLASSES OF AGNS

Four EMSS XBLs were observed by *EXOSAT*: MS 0317.0+1834, MS 1207.9+3945, MS 1235.4+6315, and MS 1402.3+0416 (Giommi et al. 1987). Spectral fits have been performed only upon the *EXOSAT* data for MS 0317.0+1834 and MS 1402.3+0416. These data were recently reanalyzed by Sambruna et al. (1994a, b), who find a spectral index

$\alpha = 1.24 \pm 0.09$ for MS 1402.3+0416. The *EXOSAT* spectrum of MS 0317.0+1834 is acceptably fitted only by a broken power law, which steepens from $\alpha = 0.67 \pm 0.11$ to $\alpha = 3.28 \pm 4.22$ at $E = 4.0 \pm 2.3$ keV (all error bars 90% confidence). Both sources' *EXOSAT* spectra are fitted by models somewhat flatter in the PSPC band; however, the results are not immediately comparable because *EXOSAT* lacked energy resolution below 2 keV. *EXOSAT* observed MS 0317.0+1834 at a flux consistent with its discovery flux (Table 2) but a factor of 6 higher than its *ROSAT* PSPC flux. The 1 keV flux for MS 1402.3+0416 obtained with *EXOSAT* is brighter by a factor of 7 than its discovery flux (Table 2), and nearly a factor of 2 brighter than its flux in the *ROSAT* PSPC observation. Thus, it is possible that these two objects follow the trend noted by Giommi et al. (1991) and harden in the soft X-rays when observed at a high state.

We have plotted the distribution of the best-fit power law indices for the PSPC spectra of our sample of XBLs in Figure 4. These data can be compared with similar data for radio-selected BL Lacs, F-R 1 radio galaxies, and radio-loud quasars, and will help to better define the relationship between BL Lacs and other types of AGNs.

3.1. *Comparisons with Earlier X-Ray Spectra of Other BL Lac Objects*

WW90 compiled *Einstein* IPC spectra of 23 RBLs and six XBLs. Until recently, their work comprised the only large sample of BL Lacs whose X-ray spectra were analyzed in a consistent way. Unfortunately, the IPC data are of limited quality, with in many cases inadequate counts collected to tightly constrain the spectral indices, particularly when both α and N_H are allowed to vary. Sambruna (1994) has partially remedied this problem by reanalyzing 14 of the IPC spectra analyzed in WW90 with N_H fixed at Galactic (Stark et al. 1992) levels. But six RBLs (not reanalyzed by Sambruna) have fewer than 100 counts and/or errors which are so large (90% confidence errors $\geq \pm 5$ in the spectral index) that the fits are essentially unconstrained (WW90). Given the higher quality of the present data, we have excluded such objects from the comparison below. We also exclude from our analysis 0521−365, which has been found to have an optical spectrum inconsistent with classification as a BL Lac by Stickel, Kühr, & Fried (1993).

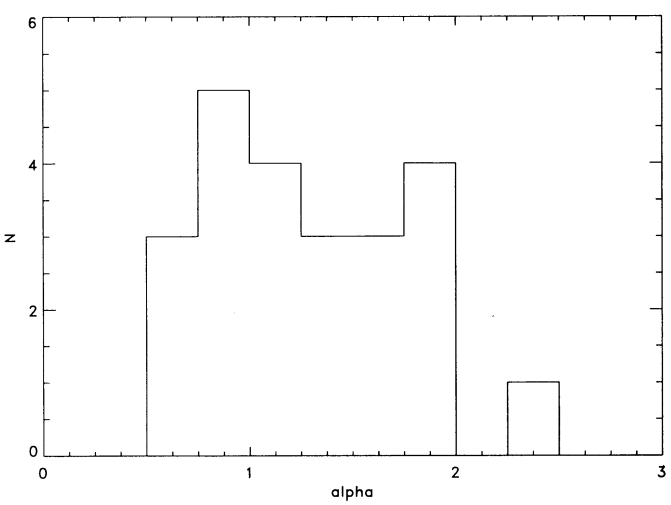

FIG. 4.—Histogram showing the distribution of energy spectral index α for the EMSS sample of X-ray selected BL Lacs in Table 1.

For the remaining objects in the WW90 sample, the arithmetic means of the RBLs is $\alpha = 0.84 \pm 0.52$, compared to $\alpha = 1.19 \pm 0.48$ for the XBLs. The two samples have weighted means of $\alpha = 0.66 \pm 0.10$ (RBL) and $\alpha = 1.18 \pm 0.10$ (XBL), respectively. But while the mean spectral index of our sample is significantly steeper than the mean index of the WW90 RBL sample, and roughly comparable to the mean index of the WW90 XBL sample, we must emphasize that given the low quality of the fits to several of the remaining RBL spectra (error bars in $\alpha \sim \pm 1$–5) and the small number of counts in several of the IPC spectra it is not possible to say definitely that the PSPC spectra analyzed here are significantly steeper than the IPC spectra of the WW90 sample.

Einstein SSS spectra of five BL Lacs (four XBLs, one RBL) were analyzed by Urry, Mushotzky, & Holt (1986). These spectra were quite steep, and some (those of PKS 0548−322 and PKS 2155−304, both of which are among the more extreme of BL Lacs in their properties) were best fitted by two power laws, with a break to flatter α near $\sim$1–2 keV. Such a break would be very difficult to detect in *ROSAT* PSPC spectra.

EXOSAT spectra of a sample of BL Lacs showed little evidence for this flattening at high energies (Barr et al. 1989; Sambruna et al. 1994a, b). For the highest count XBLs, Sambruna et al. (1994a, b) noted that only broken-power law models, with breaks in the 1–5 keV range, adequately fit the data. In all but one case, the high-energy spectral index was *steeper* than the low-energy spectral index. This may indicate that XBL X-ray spectra are dominated by the steepening tail of the particle energy distribution in the synchrotron-emitting jet, rather than flatter-spectrum inverse-Compton radiation from the radio and millimeter jet (§ 4.2). Collaborative evidence is found in Ciliegi et al. (1995) who analyze data from a variety of missions for 26 RBLs and 16 XBLs, and find that while the mean spectral index in the 2–10 keV band is steeper than that for the 0.2–4 keV band for the XBL population, the opposite is the case for the RBL population.

Urry et al. (in preparation; see also Sambruna 1994) have compiled PSPC spectra of 20 RBLs in the 1 Jy sample, and also note a trend toward steep spectra. A detailed comparison between XBL and RBL PSPC spectra will be made in that paper.

3.2. *BL Lac Objects and F-R 1 Radio Galaxies*

If BL Lac objects are F-R 1 radio galaxies seen close to the beaming axis, one would expect that the unbeamed characteristics of both should be similar. Worrall & Birkinshaw (1994) find the PSPC images of six low-power (F-R 1) radio galaxies require two-component models, in particular a resolved thermal component ($kT \sim 0.5$–1 keV) and an unresolved component (see below). For these F-R 1's, the total power of these two components is $\sim 10^{-4}$ of the X-ray powers typical of BL Lac objects, so one would not expect to be able to detect this thermal component in our BL Lac observations, and indeed we do not. The sizes and X-ray luminosities of normal elliptical galaxies (Fabbiano et al. 1984).

The point sources discovered by Worrall & Birkinshaw could be a weak isotropic synchrotron component, so it would be more relevant to compare the spectral index of the unresolved components (if nonthermal) to the mean spectral index found in our work. Unfortunately, not enough counts (< 100 in

all cases) were gathered for any one source's unresolved component to definitely determine whether it is nonthermal, much less fit a spectral index. However, when model spectra were fitted to the integrated (resolved + unresolved) counts to all sources, a combination power-law plus thermal model generated the best fits (though it should be noted that a purely thermal model also generates acceptable fits). In one case (NGC 6251) Birkinshaw & Worrall (1993) use gas confinement to argue for a nonthermal origin for the unresolved emission, rather than a hotter thermal component. Their conclusion is supported in the more general case by a fairly tight proportionality between the X-ray power-law luminosity and radio core luminosity. The power-law energy spectral indices of the nuclear sources (for the combined power-law plus thermal models of integrated emission) are very poorly determined, and range from $\alpha = -0.5$ to $\alpha = 1.4$. While these values are somewhat flatter than the indices we derive for the EMSS sample of XBLs, the errors are large enough (± 0.5 at 1 σ) that the nuclear component of F-R 1's could be weaker versions of the steep power laws we detect in XBLs. So while the detection of a weak point X-ray source component in F-R 1 radio galaxies strengthens their connection with BL Lac objects, the nature of this isotropic component is still unclear.

3.3. *BL Lacs and Radio-loud Quasars*

Based upon our data, we can confirm the preliminary conclusion based on *Einstein* IPC spectra (WW90) that BL Lacs have significantly steeper X-ray spectra than flat radio-spectrum and highly polarized quasars. Brunner et al. (1992) reported that the average *ROSAT* (energy) spectral index for a sample of 23 quasars with steep radio spectra (i.e., lobe-dominated, and perhaps less beamed; see, e.g., Padovani & Urry 1992; Ghisellini et al. 1993) was $\alpha \approx 1.35$, whereas the average value for a sample of 22 flat radio-spectrum quasars was $\alpha \approx 1.1$. The latter value is slightly flatter than the present sample, but the first is essentially identical. Unfortunately the detailed data of Brunner et al. (1992) remain unpublished so we cannot do appropriate statistical tests currently. Under viewing angle-based unified schemes, the small viewing angles $\leq 10°$ (Oppenheimer & Biretta 1994; Ghisellini et al. 1993; Padovani & Urry 1992) required for F-R 2 radio galaxies to be the parent population of radio-loud quasars makes the comparison between RBLs and radio-loud quasars much more relevant than comparisons with the XBLs we address here. Therefore, this comparison will be discussed in more detail by Urry et al. (1996).

4. THEORETICAL IMPLICATIONS OF THE STEEP X-RAY SPECTRA

4.1. *Absence of a Broad Emission-Line Region*

One of the observational hallmarks of BL Lac objects is the absence of luminous, high-equivalent width (~ 100 Å) emission lines typically seen in all other types of active galaxies. Because some blazars exhibit nearly featureless spectra at some epochs and prominent emission-line spectra typical of quasars at other times (e.g., 1308 + 326; Stickel et al. 1993), it has been suggested that BL Lacs lack emission lines due to the presence of a very luminous and potentially highly variable synchrotron continuum. However, the point source to host galaxy contrast in some RBLs (e.g., BL Lac itself) and most XBLs as measured in direct images and by optical spectroscopy is so modest that a typical quasar broad emission-line region could not be hidden by the featureless continuum (Wurtz et al. 1996; M91; Stickel et al. 1993). In particular, some XBLs possess optical spectra which reveal absorption lines whose equivalent widths are only modestly diminished by the BL Lac continuum when compared to giant elliptical galaxies (M91).

GFM83 have hypothesized that the physical conditions within the broad-line regions of BL Lacs might prevent the formation of broad-line clouds. Unlike quasars and Seyferts whose hard X-ray spectra ($\alpha \approx 0.7$) force a double-valued temperature curve as a function of ionization parameter typical of the "two-phase interstellar medium" models (i.e., warm 10^4 K clouds embedded in a 10^{7-8} K hot, diffuse medium which pressure-confines these clouds; Krolik, McKee, & Tarter 1981), the very soft X-ray spectra of BL Lacs (Fig. 4) have insufficient hard X-ray photons to heat the circumnuclear gas to $\sim 10^7$ K. The critical parameter in their hypothesis is the ratio of the number of soft (10–100 eV) photons compared to hard (≥ 1 keV) photons. Where the soft X-ray photons predominate, GFM83 showed that all the gas within $\sim 10^{18}$ cm from the nucleus will exist in a single phase at $T \leq 10^6$ K, either in the form of a fairly uniform diffuse gas, in a thin accretion disk, or in numerous, very small self-gravitating clouds. For self-gravitating clouds or for a thin accretion disk, little X-ray flux is intercepted and reradiated as emission lines. Thus for expected values of the ionization parameter (10^{2-3}) any diffuse gas will be highly ionized and so also will absorb and thus reemit little of the ambient ionizing radiation. Feedback mechanisms similar to those observed in massive X-ray binary systems (Guilbert & Fabian 1982) could "lock" the AGN circumnuclear regions into either the two-phase or single-phase state.

The GFM83 hypothesis has not been discussed recently due to two developments. First, the pressure-confined broad-line clouds envisioned by Krolik et al. (1981) are likely severely modified by ram pressure and/or magnetic cloud confinement. Thus, it is possible that warm clouds could exist in a hot medium significantly cooler than 10^7 K as required by the Krolik et al. (1981) model. Second, many BL Lacs have recently been found to be copious hard X-ray and even gamma-ray emitters (e.g., von Montigny et al. 1995).

We resurrect the GFM83 model for BL Lacs here for the following reasons:

1. Unlike Seyferts, QSRs, and QSOs, the PSPC spectra of both XBLs and RBLs are quite steep, in most cases significantly steeper than the $\alpha > 1$ required by the GFM83 model.
2. Flattening of the X-ray spectrum at $E \sim 1$–2 keV (Urry et al. 1986; Ciliegi et al. 1995; Madejski et al. 1995) has so far been observed only for bright RBLs. Further, the EGRET-detected BL Lacs are predominantly RBLs (seven of nine; an eighth, 2005 − 489, is a borderline XBL/RBL). Current data are consistent with many XBLs possessing little or no hard X-ray component (see § 4.2).
3. The weak nuclear component seen in F-R 1's (Worrall & Birkinshaw 1994; also § 3.2) is most likely a much weaker version of the soft synchrotron component we have detected for these XBLs. But regardless of its nature, these observations suggest that BL Lacs possess little ionizing radiation emanating from their nuclei at large angles from the jet axis.

We suggest the following model shown in cartoon form in Figure 5. This model can be applied only under the "viewing angle" unified scheme, as in that model, the hard X-rays produced by self-Compton processes will be beamed into a much

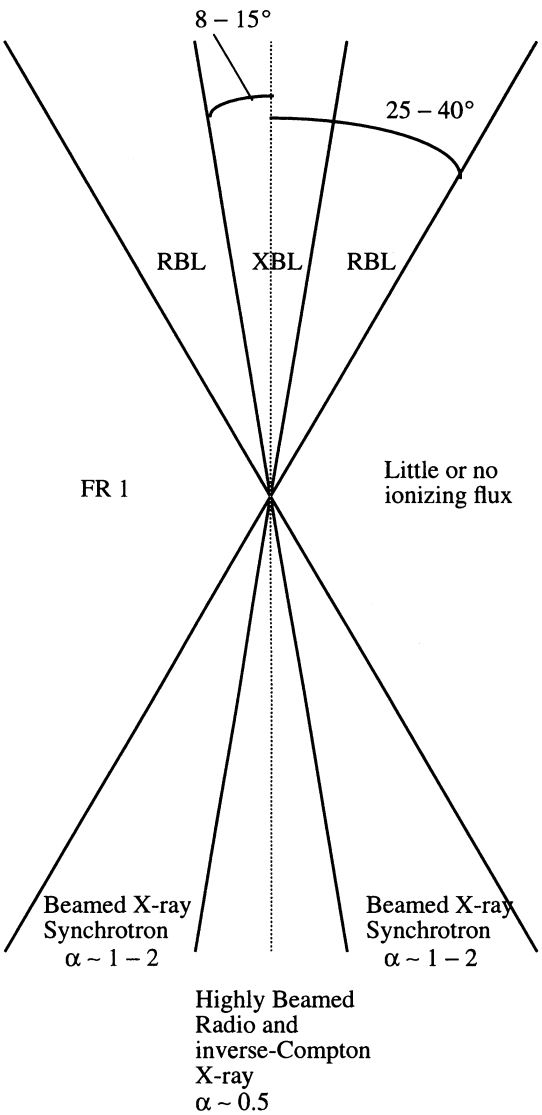

FIG. 5.—Cartoon showing the revised Guilbert, Fabian, & McCray (1983) model described in § 4.1. The I. C. abbreviation stands for inverse Compton. The angular sizes of the various regions are those suggested by previous studies mentioned in the Introduction.

smaller angle than the softer synchrotron component. Thus the putative broad-line region in BL Lacs "sees" an X-ray spectrum dominated by steep-spectrum synchrotron radiation (§ 4.2), which appears to be present in both RBLs and XBLs, or little ionizing flux at all. We speculate that a hard inverse Compton component may be present only for those BL Lacs seen close to the beaming axis and will not be detected in objects viewed well off the beaming axis (e.g., most XBLs under the "viewing angle" hypothesis).

We note that the GFM83 model does not explain why most BL Lacs lack narrow emission lines since these lines are formed in gas much farther from the nucleus ($\geq 10^{20}$ cm). A few BL Lacs do possess weak narrow emission lines (Stickel et al. 1993). Interestingly, perhaps the flattest spectrum XBL in our sample (MS 1019.0+5139) is the only EMSS XBL possessing weak emission lines.

4.2. *Synchrotron and Inverse Compton Radiation in the X-Ray Jet*

In order to test whether the soft X-ray emissions of XBLs are dominated by synchrotron of self-Compton emissions, we fitted a parabolic spectrum to our XBLs, using the total monochromatic powers at 5500 Å, and 1 keV (this paper). We then compared the slope of the tangent to the parabola at 1 keV (α_T) with our observed spectral index. This plot is shown in Figure 6. To within the errors, our X-ray spectra are either comparably steep or somewhat steeper than the tangent slope, with five exceptions: MS 0122.1+0903, MS 0419.3+1943, MS 0737.9+7441, MS 0922.9+7445, and MS 1019.0+5139 (denoted with squares in Fig. 6). These data points for each object were taken nonsimultaneously; therefore, variability could affect these numbers at some level (typical XBL optical variability is ~1 mag; Jannuzi et al. 1993. For X-ray variability see § 5.1). However, while not a physical model, the overall rough agreement of these tangent slopes and the best-fit α's suggests that, for the large majority of the objects in the complete EMSS sample, there is no evidence for any flattening within the PSPC band due to contributions from inverse Compton radiation tied to the radio/millimeter jet. The five XBLs with flat X-ray spectra may be that fraction of the EMSS XBL sample viewed closer to the radio jet axis than the remainder. Indeed, under the "viewing angle" model, one to three such objects are expected in the M91 complete EMSS sample under the viewing angle hypothesis. A similar analysis was presented by Brunner et al. (1994) for a much smaller sample of RBLs, with similar conclusions.

If our modified GFM83 model for linelessness in BL Lacs is correct, then the greater than 1 keV X-ray spectra of very off-axis BL Lacs should be quite steep, at least as steep as observed by the *ROSAT* PSPC. Those XBLs which exhibit preferred position angles of optical polarization (Jannuzi et al. 1994) are the most convincing examples of off-axis BL Lacs and so are ideal targets for this test. Unlike most RBLs, which have highly variable optical polarization position angles, ~80% of XBLs exhibit preferred position angles ($\approx \pm 10°$)

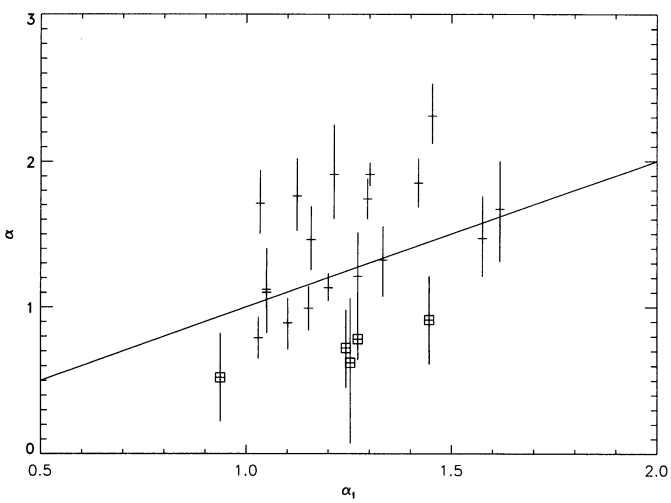

FIG. 6.—Plot of X-ray spectral index α vs. α_t, the tangent slope at 1 keV of a parabola fitted to the radio, optical, and X-ray power of each source (see § 4.2). The line denoting $\alpha = \alpha_t$ has been overplotted. The five objects for which α is significantly less than α_t have been denoted by squares. For this plot, those objects for which spectral indices were derived from RASS hardness ratios have been assigned an error in α of ±0.3.

(Jannuzi et al. 1994). Contrary to viewing a wiggling jet along its axis, an off-axis jet would create a preferred angle on the sky whose position angle would vary only slightly.

Our modified GFM83 model predicts that certain optical and/or radio jet properties will be correlated with hard X-ray properties. In particular, since self-Compton emission should be beamed into a solid angle comparable to that of the radio/millimeter jet, correlations of α at $E \gtrsim 1$ keV with radio power (log $P_{5\ \mathrm{GHz}}$), the presence (or lack thereof) of superluminal motion, and the radio core-dominance on milliarcsecond and perhaps arcsecond scale, all need to be investigated. Correlations with polarization properties (e.g., P, the maximum percent polarization in the optical and σ, the standard deviation of the optical polarization position angle) are also likely.

Preliminary verification of this hypothesis is provided by the results of Sambruna et al. (1994a), who show that *EXOSAT* XBL spectra steepen at high energies. They also present marginally significant evidence that RBL high-energy spectra are somewhat flatter than XBL high-energy spectra, though given the small sample size (16 XBLs, but only five RBLs), caution is clearly warranted. Ciliegi et al. (1995) come to similar conclusions based on a multifrequency analysis of largely pre-*ROSAT* X-ray data.

EGRET has detected six BL Lacs (0235+164, 0537−441, 0716+714, 0954+658, 1101+384, 1219+285) at $\geq 5\ \sigma$, and three more at 4–5 σ (0829+046, 1604+159, 2005−489), in the γ-rays (von Montigny et al. 1995). All but two of these objects are clearly RBLs (2005−489 is a borderline RBL/XBL, while 1101+384 is also an XBL). Strikingly, other very bright XBLs (e.g., PKS 2155−304) are not detected. Given the lower overall radio luminosity of XBLs this is not completely unexpected given the strong correlation of γ-ray and radio luminosity shown by Stecker, Salamon, & Malkan (1993); however, the ratio L_X/L_γ is significantly higher for XBLs than RBLs, causing problems for Comptonization models for the production of γ-rays in BL Lacs (Madejski et al. 1995).

5. LUMINOSITY FUNCTION AND EVOLUTION

With the data in Tables 1 and 2, we have recalculated the luminosity function and cosmic evolution for the complete EMSS sample of X-ray selected BL Lac objects. Due to the differential sky coverage of the EMSS as a function of flux, it is necessary to use the formulation of Avni & Bahcall (1980) to calculate $\langle V_e/V_a \rangle$ (instead of $\langle V/V_{\max} \rangle$), where V_e is the volume enclosed by each object and V_a is the available volume within which each object could have been detected in the EMSS. We have basically followed the Avni & Bahcall (1980) method outlined in M91, with the important extra addition that the spectral indices are now set to the values in Table 1 observed for our PSPC data and the fluxes are the rederived values in Table 2. For the purposes of the complete EMSS sample, the sky coverage given in Gioia et al. (1990b) was truncated at 5×10^{-13} ergs cm^{-2} s^{-1} and $\delta \geq -20°$, as explained in M91. While the sky coverage we have used is explicitly for sources with $\alpha = 1$, we have investigated the effects that recalculating the EMSS sky coverages for different spectral slopes would make on these results for changes in α of 0.5, and found them well below changes produced by the errors in the fluxes for individual sources. The sample used for these calculations is slightly modified from that of M91; MS 1019.0+5139 has been added as a newly recognized BL Lac (see § 5.2 for details) so that the full sample now has 23 objects.

For these calculations, we assumed density evolution of the form $\rho(z) = \rho(0)(1+z)^\beta$, and luminosity evolution of the form $L_x(z) = L_x(0)(1+z)^\gamma$, In Figure 7, we show the results of this calculation for density evolution schemes (both the luminosity function and a plot of β vs. $\langle V_e/V_a \rangle$ are shown). In Figure 8, we give the results of this calculation for luminosity evolution schemes, including both the luminosity function and a plot of γ vs. $\langle V_e/V_a \rangle$. The earlier results of M91 are also shown on these two figures for comparison. Because all differences between the present recalculation and that in M91 are minor, none of the conclusions in M91 regarding XBL luminosity function and cosmological evolution need be modified.

Using the rederived discovery fluxes for this sample (Table 2), we calculate $\langle V_e/V_a \rangle = 0.331 \pm 0.060$, and best-fit values of $\beta = -5.0$ and $\gamma = -7.0$ for the M91 EMSS sample of XBLs. Our best-fit values for β and γ are slightly less steep than (but well within the 1 σ errors of) the models calculated in M91 for density and luminosity evolution schemes, respectively. The 2 σ range for density and luminosity evolution, along with the calculated luminosity function for each, are also shown in Figures 7 and 8. The best fits to the data have strong negative evolution, i.e., XBLs were either much less common or much

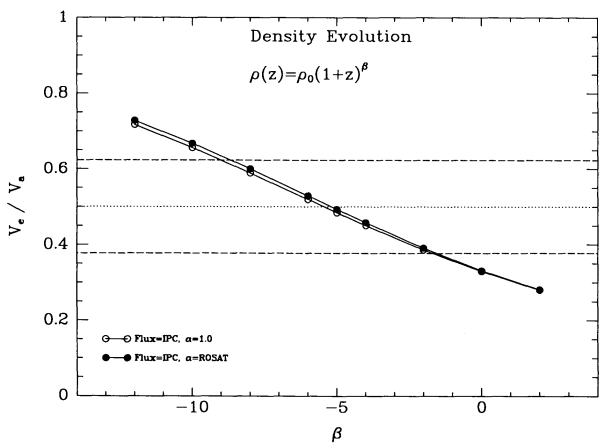

FIG. 7a

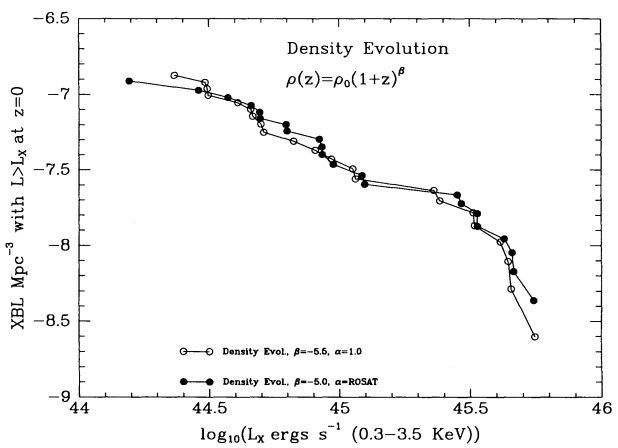

FIG. 7b

FIG. 7.—Plots of (*a*) $\langle V_e/V_a \rangle$ vs. β and (*b*) the luminosity function of XBLs assuming pure density evolution. Both the luminosity function computed herein using these *ROSAT* spectral data, and the previous luminosity function computations of M91 are shown. In part (*a*), the 2 σ limits are plotted as dashed lines.

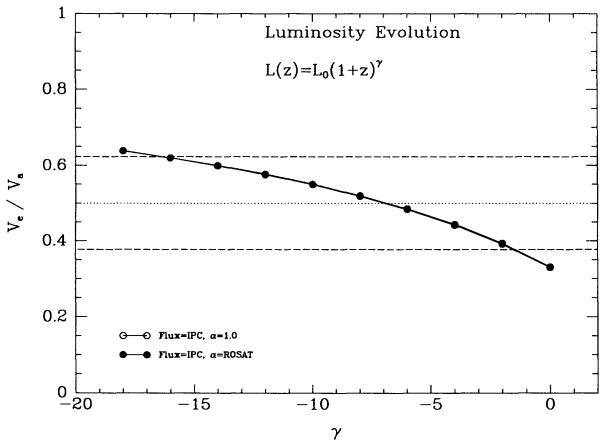

FIG. 8*a*

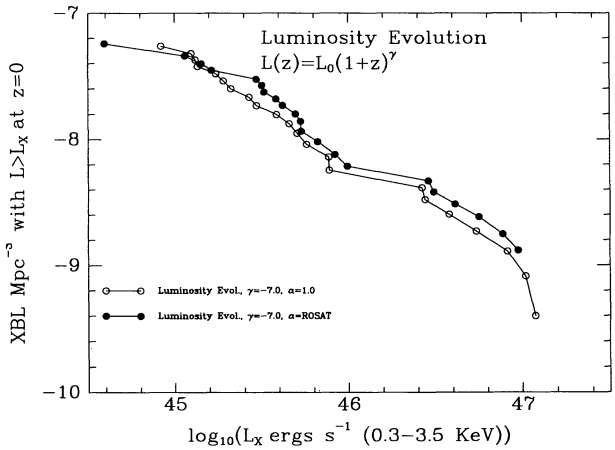

FIG. 8*b*

FIG. 8.—Plots of (*a*) $\langle V_e/V_a \rangle$ vs. γ and (*b*) the luminosity function of RBLs are shown assuming pure luminosity evolution. Both the luminosity function computed herein using the *ROSAT* spectral data, and the luminosity function computations of M91, are shown. In part (*a*), the 2 σ limits are plotted as dashed lines.

less luminous in the past than today. However, we caution the reader that due to the small number of objects and fairly small redshift range covered by these objects, the evolution is rather poorly determined.

Three objects (MS 0205.7+3509, MS 0950.9+4929, and MS 1402.3+0416) in the complete sample (as reconstituted in this paper) have uncertain redshifts. MS 0205.7+3509 is the sole BL Lac among 50 to show a decentered AGN in imaging work of Wurtz (1994). It also shows an excess N_H; our fits require a column over 4 times Galactic. For this reason, Stocke et al. (1995) have suggested that this source is a gravitational lens. The redshift of $z = 0.318$ (M91) is probably the optical "host" galaxy's redshift; therefore, this represents a lower limit on the AGN's redshift. We have attempted to isolate the redshift of the foreground galaxy and the AGN in our MMT spectrum, but so far to no avail.

The redshift of MS 0950.9+4929, as given in M91, was based on observations of a companion galaxy; we have been unable to obtain a redshift for this object, either from the M91 observation or any subsequent high signal-to-noise observation (five total attempts). This XBL is unresolved in both optical and radio (20 cm, A array) observations, leading us to believe its redshift is ≥ 0.5. We have therefore used $z = 0.5$ for these calculations. We have repeated our $\langle V_e/V_a \rangle$ calculation assuming $z = 2$ for both MS 0950.9+4929 and MS 0205.7+3509, in order to estimate the maximum effect upon the $\langle V_e/V_a \rangle$ caused by the uncertainty in their redshifts. This test produces $\langle V_e/V_a \rangle = 0.342 \pm 0.060$, so that we can safely say that the effect of assuming a larger redshift for these objects is small.

The redshift of MS 1402.3+0416 remains uncertain. Previously M91 claimed $z \approx 0.2$, based upon the detection of a spectral break, presumably due to Ca H and K. However, several attempts have failed to confirm this redshift in other lines; this redshift would also require the host galaxy to be somewhat underluminous ($M_v \geq -22$; Wurtz 1994). Recent spectra obtained by Stocke et al. (in preparation) show a tentative $z = 0.344$ using the crosscorrelation technique of Ellingson & Yee (1994). For the luminosity function calculations in this paper we have used $z = 0.344$.

5.1. *The Effect of Variability*

BL Lac objects are known for their variability in all wavebands in which they have been extensively observed. This is certainly true of this sample (e.g., Jannuzi et al. 1993) including the X-ray band. Because we have two epochs of soft X-ray observations from the *Einstein* IPC discovery of these sources and now from the *ROSAT* PSPC observations reported herein, the X-ray variability of XBLs can be crudely characterized and is shown as a histogram of percent variability in Figure 9. We define percentage variability as $100 \times [f(ROSAT) - f(Einstein)]/[f(ROSAT) + f(Einstein)]$.

Because the XBL $\log N(>S) - \log S$ curve is rather flat and only slowly changing in slope (see Fig. 2 of Wolter et al. 1991) near the flux limit of the M91 sample, we expect that the effects of source variability on the computed luminosity function and cosmological evolution will be quite small. Based upon the observed EMSS source counts and errors in those counts given in Wolter et al. (1991), the relative numbers of BL Lacs a factor of 2 above and below the M91 flux limit (a flux bin width that encompasses most of the two-epoch variability values we have observed for the M91 sample) is ~ 1.5; i.e., there is a higher differential surface density of BL Lacs just above the M91 flux limit than just below it. Given the absolute value of the BL Lac surface density at the M91 flux limit, a factor of 2 variability

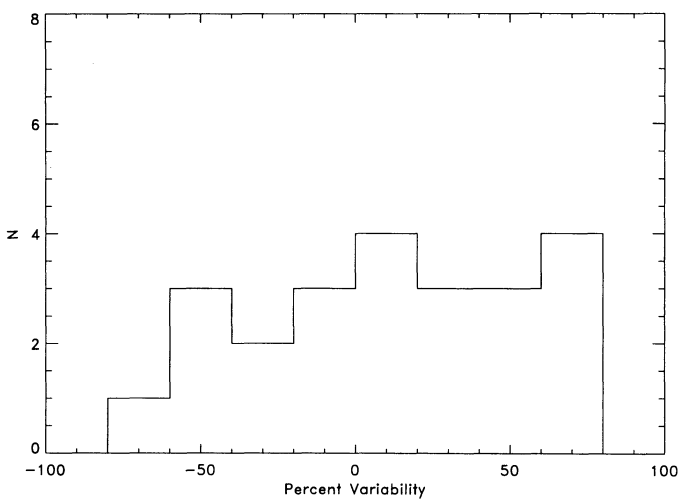

FIG. 9.—Histogram showing the distribution of percent variability in X-rays between the *Einstein* IPC and *ROSAT* observations for this sample. Percent variability is here defined as $100 \times [f(ROSAT) - f(Einstein)]/[f(ROSAT) + f(Einstein)]$.

could cause a net loss of one BL Lac from the M91 sample due to variability. This loss would cause our computed value of $\langle V_e/V_a \rangle$ to be too low by ≤ 0.03. The analysis of Wolter et al. (1994), which extends the M91 sample to a fainter flux limit but does not use our new spectral index information, suggests the same size and sense correction as mentioned here to account for variability.

5.2. *Estimated Incompleteness*

Browne & Marcha (1993) have made some interesting comments regarding the completeness of X-ray selected samples. Their contention is that, since BL Lacs lie in the nuclei of luminous elliptical galaxies, low-luminosity BL Lacs may be difficult to recognize. This would cause, for example, the EMSS sample to contain several X-ray sources misidentified as normal galaxies or clusters of galaxies rather than weak BL Lacs. This would make the EMSS sample—and other X-ray selected samples—incomplete at the low-luminosity end and skew $\langle V/V_{\rm max} \rangle$ determinations.

However, Browne & Marcha's results are based upon two important assumptions: first, that the BL Lac luminosity function extends for several orders of magnitude below the current lowest luminosity XBLs in the EMSS with the same power-law slope. While this may seem reasonable based upon the observed luminosity function of galaxies, it does not need to be the case; e.g., the luminosity function of radio-loud quasars appears to be truncated at quite high power levels (Padovani 1992a, b). Second, Browne & Marcha (1993) assume an X-ray flux limit which is a factor of 6 below the flux limit of the M91 sample. The Browne & Marcha (1993) analysis should be redone assuming the flux limit of M91 and also making various assumptions about the BL Lac luminosity function's slope at the faint end and luminosity cutoff to determine if low-luminosity BL Lacs could change the $\langle V_e/V_a \rangle$ value computed here.

In order to estimate the number of possible misidentifications that could contribute to the low value of $\langle V_e/V_a \rangle$ that we find, we have scrutinized the X-ray, optical, and radio data for the EMSS subsample used to construct the M91 XBL complete sample (i.e., $f_x \geq 5 \times 10^{13}$ ergs cm^{-2} s^{-1} and $\delta \geq -20°$). In order to directly address the concerns of Browne & Marcha (1993) we have particularly scrutinized the cluster and "normal" galaxy sources but have also scrutinized the weak-lined quasars ($W_\lambda < 50$ Å). Among the weak-lined quasars (see Table 7 in Stocke et al. 1991), there are no new BL Lac candidates to add because all EMSS quasars which are weak-lined are either below the M91 flux limit or are radio-quiet or both.

For the cluster and galaxy IDs to be suspect we have required that the X-ray source be pointlike to the IPC and that a radio galaxy be present within the area of the X-ray detection. We have excluded all sources which are well-resolved by the IPC, arguing that even if BL Lac sources are embedded within a diffuse ICM or within the nucleus of a nearby galaxy, these point sources must be weak compared to the overall extended cluster or galaxy emission. By this argument we suggest, but cannot definitively prove, that well-resolved EMSS sources are unlikely to hide a BL Lac bright enough to be included in the M91 subsample. Interestingly, despite the much better sensitivity that the *ROSAT* PSPC detector has for extended emission (due to its much lower background count rate compared to the IPC), we have detected no extended emission around any of the EMSS BL Lacs observed in this program.

Further, optical observations of a large sample of BL Lacs including the complete M91 sample have discovered only a few (five) BL Lac objects in rich clusters of galaxies (out of approximately 50; see Wurtz 1994), including two from the EMSS (MS 1207.9+3945 and MS 1407.9+5954; see Wurtz et al. 1993b). Neither of the two EMSS BL Lacs in clusters show any evidence for extended X-ray emission. However, given their high redshifts, a sensitive search with the *ROSAT* HRI should be conducted. Low-luminosity BL Lacs must be more highly correlated with rich clusters than those already identified in order for there to be many of them in the M91 EMSS subsample. Also we note that attempts to discover low-luminosity BL Lacs among cluster radio galaxies have been largely unsuccessful (Owen, Ludlow, & Keel, in preparation).

VLA snapshot observations of the EMSS sample set typical limits of $F_\nu \leq 1.0$ mJy (5 σ) at 5 GHz for all extragalactic sources with $\delta > -40°$. This limit corresponds to log $P \leq 23.5$ W Hz^{-1} at $z \leq 0.3$, below the level of most F-R 1 radio galaxies and also well below the level expected for even faint BL Lacs (Perlman & Stocke 1993; however, it should be noted that the *Einstein* Slew Survey sample contains one BL Lac object at log $P_{5\ \rm GHz} = 23.45$, out of 62 total; see Perlman et al. 1995 for details). At higher redshifts Perlman, Stocke, & Burns (in preparation) have obtained considerably deeper VLA maps of all EMSS clusters at $z \geq 0.3$ north of $-20°$. Between these two sets of observations, any potential low-luminosity BL Lac in the M91 sample would be discovered by its radio emission. Therefore, we eliminate all cluster (and normal galaxy) sources with no radio emission detected. Among the remaining sources, radio galaxies whose optical spectra exhibit strong, narrow emission lines (typically [O II] and/or Hα) are also eliminated as possible BL Lacs; these are cD galaxies in clusters with massive cooling flows as confirmed by Hα images in many cases (Donahue, Stocke, & Gioia 1992). No sources identified as normal galaxies survive the three-step screening above.

The sources which remain are listed in Table 3. These sources are quite simply those few clusters which are distant and compact enough that they were not clearly resolved by the IPC and which also contain radio galaxies. In some of these objects (Table 3) the proposed cluster appears quite poor on the sky survey plates and in two cases (MS 0011.7+0837 and MS 1050.7+4946) the Ca II spectral region of the radio galaxy has not yet been observed to determine if a weak nonthermal power-law component is present.

One object, MS 1019.0+5139, is quite unusual. In Stocke et al. (1991) this source was classified as a "cooling flow" galaxy because its optical spectrum contained low ionization, narrow emission lines similar to those seen in the central regions of cooling flow clusters, but without evidence of a rich cluster. Subsequent higher signal-to-noise ratio optical spectra reveal that the emission lines are, in fact, quite weak (W_λ(Hα and [N II]) = 8 Å, and W_λ([O II] λ3727) = 14 Å), and a *ROSAT* HRI image finds the X-ray emission to be pointlike, arguing against the cooling flow interpretation (Rector et al., in preparation). While the pointlike HRI image suggests that this object is some sort of AGN, the absence of strong, broad emission lines would make it unique among Seyferts or quasars. And while the presence of weak emission lines slightly brighter than the 5 Å limit (suggested by Stocke et al. 1991 as a BL Lac criterion) would be unique among XBLs, this emission is weak enough to make MS 1019.0+5139 similar to several 1 Jy RBLs which also have weak emission present. Therefore, we must

TABLE 3

EMSS CLUSTERS OF GALAXIES POSSIBLY HIDING A LOW-LUMINOSITY BL LACERTAE OBJECT

Object	z	Current ID	F_x (10^{-13} ergs s^{-1} cm^{-2})	log L_x (ergs s^{-1})	F_r (mJy)	log P_r (W Hz^{-1})	Comments
MS 0011.7+0837.....	0.163	CL	11.6	44.35	80.3	24.95	Wide-angle tail; cluster quite poor
MS 0433.9+0957.....	0.159	CL	13.7	44.52	43.5	24.66	Marginally resolved by IPC; head-tail source
MS 1019.0+5139.....	0.141	CL	14.4	44.18	2.4	23.30	Cluster quite poor; pointlike in *ROSAT* HRI; weak [O II], Hα
MS 1050.7+4946.....	0.140	CL	12.5	44.12	53.8	24.64	Cluster quite poor; wide-angle tail; weak Hα
MS 2301.3+1506.....	0.247	CL	5.82	44.43	2.5	23.80	Zwicky 8822

consider MS 1019.0+5139 a probable BL Lac object and have included it in the sample herein.

If we include all the objects listed in Table 3 in the M91 sample, we find that $\langle V_e/V_a \rangle = 0.356 \pm 0.056$. Thus we conclude that if some low-luminosity EMSS BL Lacs are hidden among sources currently identified with clusters and normal galaxies, their effect on the sample's $\langle V_e/V_a \rangle$ is small. *ROSAT* HRI observations of the sources in Table 3 are being obtained to test the Browne & Marcha (1993) hypothesis.

5.3. *Speculation on the $\langle V/V_{max} \rangle$ Discrepancy*

Our analysis leaves the discrepancy between the $\langle V_e/V_a \rangle$ values for XBLs and RBLs undiminished. If the parent population of BL Lacs were quasars, then the EMSS $\langle V_e/V_a \rangle$ value would be very discrepant. However, the oft-suggested BL Lac parent population are F-R 1 radio galaxies, whose evolutionary trends are not well understood in sense, much less measured accurately in amount. But F-R 1's are found in abundance in X-ray luminous clusters at $z \sim 0$ (Prestage & Peacock 1988) and Gioia et al. (1990a) and Henry et al. (1992) have found that X-ray luminous clusters have declined substantially in numbers between $z = 0$ and $z = 0.5$. Since the common environment of F-R 1's at $z = 0$ is largely absent at $z = 0.5$, it is possible that the F-R 1's are also absent. "Negative" evolution for F-R 1's between $z = 0$ and $z = 0.5$ might result, although we admit this is speculation. This trend matches the observed BL Lac evolution found for the EMSS XBL sample. If this is the case, then it is the 1 Jy sample $\langle V_e/V_a \rangle$ which is discrepant.

There are differences between the EMSS and 1 Jy BL Lac object properties which could be important for understanding the difference in $\langle V_e/V_a \rangle$. First, while the optical spectra of several of the 1 Jy BL Lacs exhibit weak emission lines (Stickel et al. 1993), just one of the EMSS XBLs (MS 1019.0+5139; see § 5.2) shows weak emission (M91). Second, while some of the 1 Jy BL Lacs have extended radio luminosities and radio powers more consistent with F-R 2 type sources (Kollgaard et al. 1992), none of the EMSS XBLs has the high radio power level and morphology of an F-R 2 (Perlman & Stocke 1993). As noted by Burbidge & Hewitt (1987), some 1 Jy and other RBLs have substantially higher redshifts than are present among XBLs. Taken together these results suggest that the 1 Jy sample may contain some examples of BL Lacs which are not beamed F-R 1 radio galaxies. If some RBLs are beamed F-R 2's, it is perhaps not surprising that the 1 Jy sample shows a trend towards positive evolution. It is well known that quasars (which, under unified schemes have F-R 2's as their parent population—see Padovani & Urry 1992) display positive evolution. Thus it is possible that the subsample of 1 Jy RBLs with F-R 2 radio characteristics are major contributors to the $\langle V/V_{max} \rangle$ result of Stickel et al. (1991). However not all the RBLs in the 1 Jy sample have been well-imaged with the VLA, so it is not possible to fully evaluate this effect.

While through high-resolution imaging at radio and optical frequencies we have found only one candidate for a gravitationally lensed XBL (MS 0205.7+3509; Wurtz et al. 1993a; Stocke et al. 1995), several of the 1 Jy sample have not been well-imaged optically. The presence of gravitationally lensed quasars (e.g., AO 0235+164; Stickel et al. 1988) within the 1 Jy sample of BL Lacs could cause a higher value of $\langle V/V_{max} \rangle$ for that sample. However, over $\frac{1}{3}$ of the 1 Jy sample would need to be gravitationally lensed or beamed quasars, instead of F-R 1's, to alter the $\langle V/V_{max} \rangle$ statistic by the amount needed to explain the XBL/RBL difference (see the simulations by Turner 1980 and Peacock 1986 for calculations addressing the effect of gravitationally lensed objects upon the $\langle V/V_{max} \rangle$ statistic).

Finally, we note that the 1 Jy sample selection criteria were somewhat different from those used for the EMSS; this may have caused selection effects. These differences are (1) the lack of an H and K break strength criterion; and (2) the requirement that $\alpha_r \leq 0.5$, within the selection process for the 1 Jy sample of BL Lacs. We briefly consider the effects of each difference below.

The lack of an H and K break strength criterion in the 1 Jy sample could cause some 1 Jy objects to be misidentified as radio galaxies when in fact they are low-luminosity BL Lacs. Unfortunately, no comprehensive compilation of 1 Jy identification spectra exist in the literature, so the exact magnitude of this effect is hard to gauge. However, this point may be more clearly illustrated by considering two objects identified as radio galaxies within the S4 and S5 sample, respectively: S4 1833+653 and S5 1807+707 (Stickel & Kühr 1993; Stickel et al. 1993). The S4 and S5 sample used identical criteria to those used by Stickel et al. (1991) for the 1 Jy sample. Examining the spectra of S4 1833+653 and S5 1807+707 reveals that both lack emission lines ≥ 5 Å, and both have H and K breaks of less than 25%. Thus by our criteria, they clearly qualify as BL Lac objects; however, as already noted, they were excluded from the S4 and S5 samples of BL Lacs (Stickel & Kühr 1994). Another possible example is that of the 1 Jy radio source 1721−026. Stickel et al. (1993) correctly note that the identification of a 15th magnitude galaxy at $z = 0.033$ with this radio source is controversial; however, they fail to note that if the identification is correct, it would qualify as a BL Lac object.

Thus we find significant reason to suspect that some radio galaxies in the 1 Jy catalog have been misidentified and are in reality low-luminosity BL Lac objects.

In addition, the requirement that $\alpha_r \leq 0.5$ may also have eliminated some low-luminosity BL Lacs from the sample. Stickel et al. (1991) used this criterion to eliminate the large number of radio galaxies in the catalog. But as shown in Stocke et al. (1985) some XBLs have steeper radio spectra than this limit so that some BL Lacs may have been systematically eliminated. Given that the radio cores of BL Lacs have flatter spectral indices than the extended regions (e.g., Saikia et al. 1987), this criteria would have biased the 1 Jy sample against including objects with low core-dominances. Indeed, S4 1833+653 and S5 1807+707 (see above) would both be rejected as possible BL Lac objects by this criterion. Unfortunately, spectral index data do not exist for the EMSS sample, so we cannot test the effect upon the EMSS $\langle V_e/V_a \rangle$ of adding a flat radio-spectrum criterion. Clearly, further work is needed to resolve the $\langle V_e/V_a \rangle$ discrepancy between these two samples.

6. CONCLUSIONS

We have presented *ROSAT* PSPC X-ray spectra of all 23 objects in the complete EMSS sample of BL Lac objects. The spectra are well-fitted by single power laws with indices between $\alpha = 0.5$–2.3 RBL PSPC spectra (Sambruna 1994; Urry et al. 1996) are similarly steep.

The steep spectra suggest that XBL continua in the PSPC band are dominated by the high-energy tail of synchrotron emission from the X-ray emitting jet, rather than harder, flat-spectrum inverse Compton emission directly tied to the radio and millimeter jet emission. This revives the model suggested by GFM83 who suggested that BL Lacs do not possess broad-line regions because their steep-spectrum X-ray continuum would have insufficient high-energy photons to heat the circumnuclear gas to $\sim 10^7$ K. Thus, a two-phase medium is inhibited and stable broad-line clouds cannot form. This model is most consistent with the "viewing angle" model (e.g., Stocke et al. 1989) since it requires the solid angle illuminated by the flat-spectrum inverse-Compton component to be smaller than that illuminated by the soft, steeper spectrum synchrotron component observed in these XBLs.

We have also recomputed the X-ray luminosity function and cosmological evolution for this sample of objects, by taking into account the different spectral indices for the sources which we have observed. We confirm the conclusion of M91 that X-ray selected BL Lacertae objects evolve "negatively," i.e., they are either more luminous in the present epoch than in the past, or they are more numerous now. Including the *K*-corrections using the PSPC derived spectral slopes, the best estimates on the effects of variability (based upon the soft X-ray variability amounts actually observed for this sample) and possible incompleteness in the M91 sample (we add one new XBL to the M91 sample), we find a best value of $\langle V_e/V_a \rangle = 0.331 \pm 0.060$. By contrast, the 1 Jy radio-selected BL Lac sample has $\langle V_e/V_a \rangle = 0.60 \pm 0.05$ (Stickel et al. 1991); thus the discrepancy between the $\langle V/V_{\max} \rangle$ statistics of RBLs and XBLs remains a significant problem for unified schemes. While we speculate that the 1 Jy RBL sample may include objects which are not beamed F-R 1's (as also pointed out by Kollgaard et al. 1992) and also that both samples could suffer from some incompleteness, it is not clear whether these effects will bring the discrepant $\langle V/V_{\max} \rangle$ values into agreement or not.

We thank the MPE *ROSAT* group, and in particular Thomas A. Fleming and Silvano Molendi, for communicating results from the *ROSAT* All-Sky Survey before publication. We also thank H.-C. Thomas for allowing us to quote his results on MS 1235.4+6315 in advance of publication. Finally, we would like to thank Tommaso Maccacaro and Anna Wolter for many very interesting conversations which helped this paper significantly, and for assistance in obtaining the RASS data.

This research has also made use of data obtained through the High Energy Astrophysics Science Archive Research Center Online Service, provided by the NASA/Goddard Space Flight Center. Support for ground and space-based observations of BL Lacs at the University of Colorado is funded by NASA LTSA grant NAGW-2645 and NSF grant AST-90200008. E. S. P. acknowledges support from a NASA Graduate Student Researchers' Program Fellowship (GSRP) while at the University of Colorado. Q. D. W. acknowledges support from the Lindheimer Fellowship and from NASA under grant NAG 5-1879. We would also like to thank the referee for a careful reading of the manuscript and comments which have helped improve this paper.

REFERENCES

Abraham, R. G., McHardy, I. M., & Crawford, C. S. 1991, MNRAS, 252, 482
Abramowitz, M., & Stegun, I. A. 1964, Handbook of Mathematical Functions (New York: Dover)
Antonucci, R. R. J. 1993, ARA&A, 31, 473
Avni, Y., & Bahcall, J. N. 1980, ApJ, 235, 694
Barr, P., Giommi, P., Pollock, A., Tagliaferri, G., Maccagni, D., & Garilli, B. 1989, in BL Lac Objects, ed. L. Maraschi, T. Maccacaro, & M.-H. Ulrich (Heidelberg: Springer-Verlag), 290
Bevington, P. R., & Robinson, D. K. 1992, Data Reduction and Error Analysis for the Physical Sciences (New York: McGraw-Hill)
Birkinshaw, M., & Worrall, D. M. 1993, ApJ, 412, 568
Blandford, R., & Konigl, A. 1979, ApJ, 232, 34
Browne, I. W. A. 1983, MNRAS, 204, 23P
———. 1989, in BL Lac Objects, ed. L. Maraschi, T. Maccacaro, & M.-H. Ulrich (Heidelberg: Springer-Verlag), 401
Browne, I. W. A., & Marcha, M. J. M. 1993, MNRAS, 261, 795
Brunner, H., Friedrich, P., Zimmermann, H. U., & Staubert, R. 1992, in X-Ray Emission from AGN and the X-Ray Background, ed. W. Brinkman & J. Trumper (MPE report 235), 198
Brunner, H., Lamer, G., Worrall, D. M., & Staubert, R. 1994, A&A, 287, 436
Burbidge, G., & Hewitt, A. 1987, AJ, 92, 1
Celotti, A., Maraschi, L., Ghisellini, G., Caccianiga, A., & Maccacaro, T. 1993, ApJ, 416, 118
Ciliegi, P., Bassani, L., & Caroli, G. 1995, ApJ, 439, 80
Donahue, M., Stocke, J. T. S., & Gioia, I. M. 1992, ApJ, 385, 49
Ellingson, E., & Yee, H. K. C. 1994, ApJS, 92, 33
Ellingson, E., Yee, H. K. C., & Green, R. 1991, ApJ, 371, 49
Elvis, M., Lockman, F. J., & Fassnacht, C. 1994, ApJS, 95, 413
Elvis, M., Wilkes, B. J., & Lockman, F. J. 1989, AJ, 97, 777
Fabbiano, G., Miller, L., Trinchieri, G., Longair, M., & Elvis, M. 1984, ApJ, 277, 115
Fanaroff, B. L., & Riley, J. M. 1974, MNRAS, 167, 31P
Ghisellini, G., & Maraschi, L. 1989, ApJ, 340, 181
Ghisellini, G., Padovani, P., Celotti, A., & Maraschi, L. 1993, ApJ, 407, 65
Gioia, I. M., Henry, J. P., Maccacaro, T., Morris, S. L., Stocke, J. T., & Wolter, A. 1990a, ApJ, 356, L35
Gioia, I. M., Maccacaro, T., Schild, R., Wolter, A., Stocke, J., Morris, S., & Henry, J. P. 1990b, ApJS, 72, 567
Giommi, P., Ansari, S. G., & Micol, A. 1995, A&AS, 109, 267
Giommi, P., Barr, P., Garrilli, B., Gioia, I. M., Maccacaro, T., Maccagni, D., & Schild, R. 1987, ApJ, 322, 662
Giommi, P., & Padovani, P. 1994, MNRAS, 268, L51
Giommi, P., et al. 1991, ApJ, 378, 77
Guilbert, P. W., & Fabian, A. C. 1982, Nature, 296, 226
Guilbert, P. W., Fabian, A. C., & McCray, R. 1983, ApJ, 266, 466 (GFM83)
Hasinger, G., Turner, T. J., George, I. M., & Boese, G. 1992, NASA/GSFC/OGIP, Calibration Memo CAL/ROS/92-001
Henry, J. P., Gioia, I. M., Maccacaro, T., Morris, S. L., Stocke, J. T., & Wolter, A. 1992, ApJ, 386, 408
Jannuzi, B. T., Smith, P., & Elston, R. 1993, ApJS, 85, 265

Jannuzi, B. T., Smith, P., & Elston, R. 1994, ApJ, 428, 130
Kollgaard, R. I., Wardle, J. F. C., Roberts, D. H., & Gabuzda, D. C. 1992, AJ, 104, 1687
Krolik, J. H., McKee, C. F., & Tarter, C. B. 1981, ApJ, 249, 422
Maccacaro, T., Gioia, I. M., Maccagni, D., & Stocke, J. T. 1984, ApJ, 284, L23
Maccacaro, T., Wolter, A., McLean, B., Gioia, I. M., Stocke, J. T., Della Ceca, R., Burg, R., & Faccini, R. 1994, Astrophys. Lett. Comm., 29, 267
Madejski, G. M., & Schwartz, D. A. 1989, in BL Lac Objects, ed. L. Maraschi, T. Maccacaro, & M.-H. Ulrich (Heidelberg: Springer-Verlag), 267
Madejski, G., Takahashi, T., Tashiro, M., Kubo, H., Hartmann, R., Kallmann, T., & Sikora, M. 1995, ApJ, submitted
Mattox, J. R., et al. 1993, ApJ, 410, 609
Morris, S. L., Stocke, J. T., Gioia, I. M., Schild, R. E., Wolter, A., Maccacaro, T., & Della Ceca, R. 1991, ApJ, 380, 49 (M91)
Oppenheimer, B. R., & Biretta, J. A. 1994, AJ, 107, 892
Padovani, P. 1992a, MNRAS, 257, 404
———. 1992b, A&A, 256, 399
Padovani, P., & Giommi, P. 1995, ApJ, 444, 567
Padovani, P., & Urry, C. M. 1990, ApJ, 356, 75
———. 1991, ApJ, 368, 373
———. 1992, ApJ, 387, 449
Peacock, J. A. 1986, MNRAS, 223, 113
Perlman, E. S. 1994, Ph.D. thesis, Univ. of Colorado, Boulder
Perlman, E. S., Jannuzi, B. T., Stocke, J. T., & Elston, R. in preparation
Perlman, E. S., & Stocke, J. T. 1993, ApJ, 406, 430
———. 1994, AJ, 108, 56.
Perlman, E. S., Stocke, J. T., & Burns, J. O. in preparation
Perlman, E. S., et al. 1995, ApJS, in press
Perlman, E. S., Stocke, J. T., Shaffer, D. B., Carilli, C. L., & Ma, C. 1994, ApJL, 424, 69
Prestage, R. M., & Peacock, J. A. 1988, MNRAS, 230, 131
Saikia, D. J., Salter, C. J., Neff, S. G., Gower, A. C., Sinha, R. P., & Swarup, G. 1987, MNRAS, 228, 203
Sambruna, R. M. 1994, Ph.D thesis, SISSA/ISAS, Trieste
Sambruna, R. M., Barr, P., Giommi, P., Maraschi, L., Tagliaferri, G., & Treves, A. 1994a, ApJ, 434, 468
———. 1994b, ApJS, 95, 371
Schachter, J. F., et al. 1993, ApJ, 412, 541
Schwartz, D. A., & Ku, W. H.-M. 1983, ApJ, 266, 459
Stark, A. A., Gammie, C. F., Wilson, R. W., Bally, J., Linke, R. A., Heiles, C., & Hurwitz, M. 1992, ApJS, 79, 77
Stecker, F. W., Salamon, M. H., & Malkan, M. A. 1993, ApJ, 410, L71
Stickel, M., Fried, J. W., & Kühr, H. 1988, A&A, 198, L13
———. 1989, A&AS, 80, 103
———. 1993, A&AS, 98, 393
Stickel, M., & Kühr, H. 1993, A&AS, 100, 395
———. 1994, A&AS, 103, 349
Stickel, M., Kühr, H., & Fried, J. W. 1993, A&AS, 97, 483
Stickel, M., Padovani, P., Urry, C. M., Fried, J. W., & Kühr, H. 1991, ApJ, 374, 431
Stocke, J., Liebert, J., Schmidt, G., Gioia, I., Maccacaro, T., Schild, R., Maccagni, D., & Arp, H. 1985, ApJ, 298, 619
Stocke, J., Morris, S., Gioia, I., Maccacaro, T., Schild, R., & Wolter, A. 1989, in BL Lac Objects, ed. L. Maraschi, T. Maccacaro, & M.-H. Ulrich (Heidelberg: Springer-Verlag), 242
Stocke, J. T., Morris, S. L., Gioia, I. M., Maccacaro, T., Schild, R., Wolter, A., Fleming, T. A., & Henry, J. P. 1991, ApJS, 76, 813
Stocke, J. T., Wurtz, R. E., & Perlman, E. S. 1995, ApJ, in press
Turner, E. L. 1980, ApJ, 242, L135
Urry, C. M., Mushotzky, R. F., & Holt, S. S. 1986, ApJ, 305, 369
Urry, C. M., Padovani, P., & Stickel, M. 1991, ApJ, 382, 501
Urry, C. M., Sambruna, R. M., Worrall, D. M., Kollgaard, R. I., Feigelson, K. D., Perlman, E., & Stocke, J. 1996, ApJ, in press
Vermeulen, R., & Cohen, M. 1994, ApJ, 430, 467
von Montigny, C., et al. 1995, ApJ, 440, 525
Wolter, A., Caccianiga, A., Della Ceca, R., & Maccacaro, T. 1994, ApJ, 433, 29
Wolter, A., Gioia, I. M., Maccacaro, T., Morris, S. L., & Stocke, J. T. 1991, ApJ, 369, 314
Worrall, D. M., & Birkinshaw, M. 1994, ApJ, 427, 134
Worrall, D. M., & Wilkes, B. J. 1990, ApJ, 360, 396 (WW90)
Wurtz, R. 1994, Ph.D. thesis, Univ. Colorado, Boulder
Wurtz, R., Ellingson, E., Stocke, J. T., & Yee, H. 1993, in The Evolution of Galaxies and Their Environment, ed. H. Thronson & J. M. Shull (Dordrecht: Reidel), 303
Wurtz, R., Stocke, J. T., Ellingson, E., & Yee, H. K. C. 1993b, AJ, 106, 869
———. 1996, in press

Note added in proof.—W. T. Vestrand, W. G. Stacy, and P. Sreekumar (ApJ, submitted [1996]) have detected PKS 2155−304 at GeV energies with EGRET, while T. Weeks et al. (Third Compton Symposium, in press [1995]) have now detected Mrk 501 at TeV energies.